Discrimination between softwood and hardwood based on hemicellulose content obtained with portable nuclear magnetic resonance

Valeria Stagno · **Sara Ricci** · **Sveva Longo** ·
Elena Verticchio · **Francesca Frasca** ·
Anna Maria Siani · **Silvia Capuani**

Abstract Wood is a hygroscopic material that can reach an equilibrium moisture content when ambient temperature and relative humidity are constant. Moisture affects all properties of wood, as well as its preservative treatment. The hygroscopic behavior of wood can be attributed to the hydroxyl groups of its constituents. Since hemicellulose shows the greatest water affinity, it can be considered the main responsible for the ingress of water into the wood mass. Below the fiber saturation point, wood moisture is only stored in the cell walls. Proton Nuclear Magnetic Resonance (NMR) is a relative method used for the evaluation of moisture content distribution in wood and NMR relaxation is an excellent tool to study the hygroscopic behavior of different woods below the fiber saturation point. This work aimed to test the hypothesis of discriminating among softwoods and hardwoods of different botanical species and identifying further sub-clusters of woods based on the NMR proton spin–spin (T_2) and spin–lattice (T_1) relaxation times of their cell wall water in the hygroscopic moisture range. Importantly, the study was performed using a portable low-cost NMR instrument with which it is possible to investigate wood samples of any size. The main result of this study was that at RH = 94% the relaxation time $T_{2,2}$, associated with the cell wall bound water, can be used as a marker to discriminate among softwoods and hardwoods.

V. Stagno (✉) · E. Verticchio
Department of Earth Sciences, Sapienza University of Rome, Piazzale Aldo Moro 5, 00185 Rome, Italy
e-mail: valeria.stagno@uniroma1.it

V. Stagno · S. Capuani
National Research Council-Institute for Complex Systems (CNR-ISC), c/o Physics Department, Sapienza University of Rome, Piazzale Aldo Moro 5, 00185 Rome, Italy

S. Ricci
Department of Environmental Biology, Sapienza University of Rome, Piazzale Aldo Moro 5, 00185 Rome, Italy

S. Longo
National Research Council - Istituto Di Scienza Per Il Patrimonio Culturale (CNR-ISPC), Via Madonna del Piano 10, 50019 Sesto Fiorentino, Florence, Italy

F. Frasca · A. M. Siani
Department of Physics, Sapienza University of Rome, Piazzale Aldo Moro 5, 00185 Rome, Italy

Graphical abstract
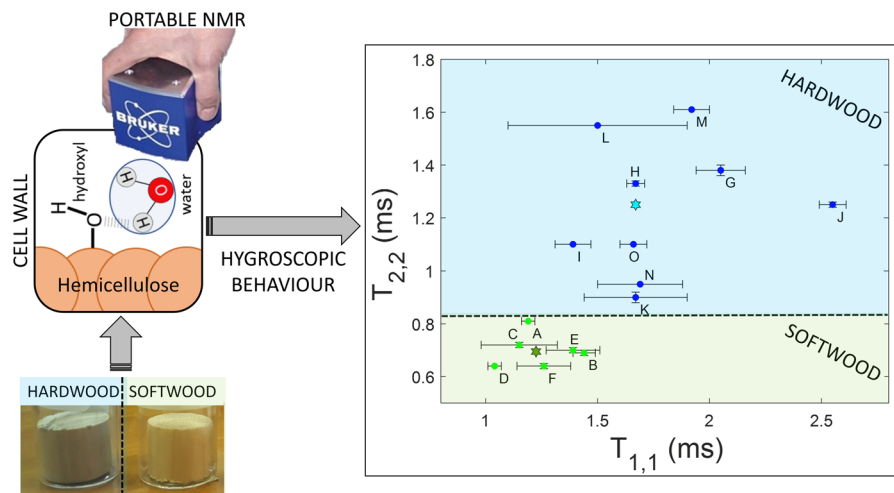
Introduction

Wood is a biological heterogeneous and anisotropic porous material (Capuani et al. 2020). It is characterized by fibers with a cell wall composed of natural polymers, such as cellulose, hemicellulose, and lignin. Among them, cellulose can be considered the most abundant component of wood (Alesiani et al. 2005). Wood can be also described as a porous system with strongly variable and multi-scale porosity. In particular, each wooden species has pores, such as pits, perforations, and the lumen of vessels, tracheids, and fibers, with peculiar dimensions and spatial organization (Capuani et al. 2020; Stagno et al. 2021a).

Wood is classified as softwood and hardwood. Softwood has a quite homogeneous microstructure mostly dominated by one kind of structure, called tracheid (Capuani et al. 2020; Stagno et al. 2021a). Different from softwood, hardwood has more complex anatomical features and greater structural variation (Stagno et al. 2021a). Indeed, its microstructure is made up of conducting elements, i.e. vessels, and strength-giving elements, i.e. fibers.

Furthermore, due to its hygroscopicity, wood can absorb moisture from the surrounding environment in the form of vapor or liquid water. Moisture affects all properties of wood. While moisture in the cell lumens only produces an increment of weight (Tsoumis

1991), moisture contained in cell walls influences the mechanical and thermal properties of wood (Bartolucci et al. 2021). Moisture content (MC) of wood also affects its resistance to decay and insects as well as its preservative treatment (Tsoumis 1991). At constant temperature (T) and relative humidity (RH), wood reaches an equilibrium state characterized by a certain equilibrium moisture content (EMC) (Glass Samuel and Zelinka 2010). A sorption isotherm is a discrete representation of equilibrium moisture states of wood with its surrounding environment and each state is attained after either adsorption or desorption of water molecules (Engelund et al. 2013).

A central role in the hygroscopic behavior of wood can be ascribable to the hydroxyls of its constituents. Cellulose and hemicellulose have a higher content of hydroxyl groups than lignin. However, because cellulose is mostly in crystalline form that is not accessible to water, hemicellulose is considered to have a greater affinity to water (Schirarend 1986; Berry and Roderick 2005; Kulasinski et al. 2015). So, hydroxyl groups of hemicellulose catch water molecules by forming hydrogen bonds and are responsible for moisture entering the wood mass. Since softwoods and hardwoods show a different hemicellulose content, i.e. hardwoods have more hemicellulose than softwoods (Holtzapple 2003; García Esteban et al. 2005), distinct hygroscopic behavior of their cell walls is expected (Elder and Houtman 2013). When dried wood is taken

at room temperature, at least a monomolecular layer of water is bonded to its constituents (Chami Khazraji and Robert 2013) and, its cell walls start swelling. Then, other water molecules align above those associated with the hydroxyl groups and form H-bonds (Berry and Roderick 2005). The result is a water polymolecular layer. An additional part may enter by capillarity condensation in the cell wall voids and pits but, it is considered insignificant below 99.5% RH (Thygesen et al. 2010). The fiber saturation point (FSP) is the moisture content that occurs when cell walls are saturated with water and cell lumens are empty. At this point, cell walls stop swelling and, the strength of the timber no longer changes with the moisture content (Berry and Roderick 2005). Below the FSP, only bound water is present in wood, and water in the smaller pores of cell walls shows a switching behavior between liquid and vapor phases (Beckstein and Sansom 2003). Above the FSP, water starts filling cells lumens as free water. Conventionally, the FSP is set around 30% of wood moisture content. However, it can also be considered as the wood EMC when RH is close to 100% (Berry and Roderick 2005).

The EMC is also affected by the wood sample history and, this phenomenon is known as sorption hysteresis. As an example, when a greenwood sample is dried, its EMC reached for adsorption will be lower than its EMC attained for desorption (Glass Samuel and Zelinka 2010). Furthermore, it has been noticed that around 60–70% RH, the sorption isotherm of wood exhibits an upward bend. This behavior can be explainable by the softening of amorphous polymers (Olsson and Salmén 2004; Engelund et al. 2013). During softening, the viscosity and rigidity of the wood polymeric network are reduced because of the transition of its amorphous parts from a glassy state to a rubbery state (Engelund et al. 2013). Due to this process, the cell wall capacity of accommodating water molecules might increase. At room temperature, softening of hemicelluloses occurs around 75% RH (Olsson and Salmén 2004; Engelund et al. 2013).

Nuclear Magnetic Resonance (NMR) is a relative method used for the evaluation of moisture content distribution in wood and masonry (Camuffo 2018). Compared to traditional relative methods for moisture content evaluation, the main advantages of NMR are the accuracy in moisture content determination and the greater penetration depth (European Committee for Standardization 2017).

In this work we used Portable Low-Field Nuclear Magnetic Resonance (LF-NMR). Indeed, although portable NMR does not allow to perform high-resolution measurements and imaging, it can be used to measure the relaxation times of wood objects in situ and in a non-invasive way.

In the past, portable NMR has been used to study different water compartments within the wood structure with particular interest for the over-hygroscopic range where water can be found not only in the cell wall but also in cell lumina and other voids with different sizes (Fredriksson and Thygesen 2017; Stagno et al. 2021c). These studies (Menon et al. 1987; Araujo et al. 1992; Labbé et al. 2002, 2006; Almeida et al. 2007; Thygesen and Elder 2009; Elder and Houtman 2013; Fredriksson and Thygesen 2017; Stagno et al. 2020, 2021c) highlighted the LF-NMR potential in characterizing water compartments of wood for probing its different anatomical elements. On the other hand, water in wood in the hygroscopic range (i.e. below the FSP) is only located in the cell wall compartment but the magnetization decay can provide information on molecular mobility expressed as spin–spin relaxation time T_2 and spin–lattice relaxation time T_1 (Thygesen and Elder 2009), which are a measure of how tight the water is bound (Fredriksson and Thygesen 2017) and of the interactions with the wood polymers. For this reason, the cell wall water has also been studied by NMR relaxation times and separated into tightly bound to macromolecules and less bound to cell walls (Casieri et al. 2004; Fantazzini et al. 2006; Thygesen and Elder 2009; Bonnet et al. 2017; Rostom et al. 2020). All the aforementioned works pointed out that water is an excellent probe of wood characteristics because it is sensitive to wood ultrastructure. Moreover, water features in wood can be used to assess the wood morphology and hygroscopic behavior.

This work aimed to exploit the possibility to discriminate among different wood samples belonging to softwood and hardwood groups and identify possible sub-clusters of woods on the base of NMR relaxation of their cell wall water in the hygroscopic range. Towards this goal, a portable LF-NMR instrument was used to develop a specific non-invasive NMR protocol for in situ investigation useful in the wood industry and/or cultural heritage applications.

Table 1 Botanical species and common name of the samples, their densities, EMC at RH = 94% and wood group softwood (S) or hardwood (H)

Botanical species	Commonname	Density (kg/m^3)	EMC (%)	Wood group
Mitragyna ciliata	Bahia walnut	530 ± 40	19	H
Populus alba	White poplar	480 ± 40	17	H
Picea abies	Red spruce	540 ± 40	17	S
Abies alba	Russian silver fir	530 ± 40	17	S
Aningeria altissima	Akatio walnut	560 ± 40	17	H
Abies alba	European silver fir	350 ± 30	18	S
Quercus petraea	Sessile oak	630 ± 50	16	H
Juglans nigra	English walnut	680 ± 50	15	H
Aningeria altissima	Tanganyika walnut	520 ± 40	15	H
Entandrophragma cylindricum	Sapele mahogany	550 ± 40	14	H
Toona ciliata	Australian red cedar	520 ± 40	17	S
Pinus ponderosa	European Virginia pine	510 ± 40	16	S
Lovoa trichilioides	African walnut	550 ± 40	20	H
Picea rubens	American red spruce	520 ± 40	16	S
Pinus ponderosa	American Virginia Pine	530 ± 40	16	S
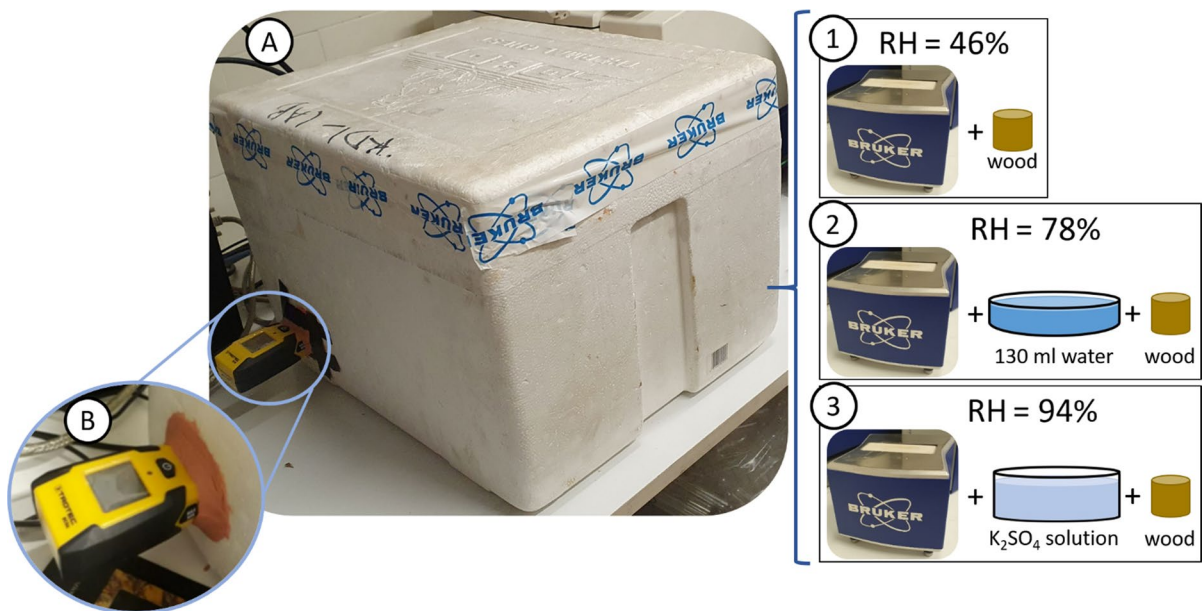
Fig. 1 Schematic representation of the climatic chamber composed by **A** a sealed Styrofoam box with (**B**) the TROTEC BC06 thermo-hygrometer used to monitor RH and T. In case (1) where RH was 46% only the NMR mouse and the wood samples were placed inside the chamber, whereas in case (2) a container with 130 ml of water was added to reach an RH = 78% and in case (3) a saturated saline solution of K_2SO_4 was used to reach RH = 94%

Experimental

Materials

Fifteen cylinder-like wood samples (Table 1) of 2.5 cm in height and 3 cm in diameter were studied. First, the green

wood samples were cut from contemporary trees and the fifteen different wood species were chosen among those most used for the production of the artworks. The woods were not cut either from the heartwood or from the reaction wood. Then, the samples were dried inside the Universal Memmert Oven stove at a temperature (T) of

103.5 ± 0.5 °C for 24 h. Their botanical species and their common name are reported in Table 1.

Since in this study NMR acquisitions were performed at different RH levels and NMR signal acquired by portable NMR Bruker instrument is particularly sensitive to little RH variations, a climate chamber was realized by using a Styrofoam box with inner volume 43 × 36 × 30 (h × l × w) cm³ (see Fig. 1). Styrofoam was chosen because of its insulating properties to prevent vapor exchanges with the external environment. Indeed, according to Nilsson et al. (Nilsson 2018), a climate chamber is recommended to maintain temperature stability because temperature fluctuation of ± 0.1 °C may produce an RH change of ± 0.5%. To keep the box temperature constant, the air conditioning system set at T = 23 °C was turned on during all the experiments time. In this way all measurements were performed by inserting the wood samples inside the box at a selected value of relative humidity and constant temperature of T = 23 ± 1 °C, which were monitored by using the TROTEC BC06 thermo-hygrometer with accuracy ± 1 °C within the range 0° to 40 °C and ± 3.5% within the range 20–80 °C.

In a first phase, four samples corresponding to Russian silver fir, European Virginia pine, akatio walnut, and white poplar (see Table 1) were equilibrated at three levels of relative humidity equal to RH = 46.0 ± 3.5%, 78.0 ± 3.5% and 94.0 ± 3.5%, while in a second phase all the samples were equilibrated at RH = 94% (see Fig. 1). RH = 46% was the environmental relative humidity of the laboratory. RH = 78% was obtained by adding in the box a container with 130 ml of liquid water. RH = 94% was reached by using a saturated saline solution of potassium sulfate (K_2SO_4) (Nilsson 2018). It is important to notice that, without considering the sample history (Glass Samuel and Zelinka 2010), the EMC of wood at the three RH levels can be predicted by the EMC calculation table (Noack 1989; W.T. Simpson 1998; Glass Samuel and Zelinka 2010) and it is expected to be approximately 9%, 15%, and 24%, respectively.

Methods

Wood density and EMC

Average dry weight values by gravimetric method (Noack 1989) were obtained for each wood species. Masses of all dried wood samples were measured

with an analytical balance BP211D Sartorius and their volume was calculated. Then, the density of each sample was expressed in kg/m³. Moreover, the weight of the fifteen samples equilibrated at RH = 94% was measured and used to calculate the relative equilibrium moisture content (EMC).

NMR relaxometry

The NMR relaxometry measurements were performed using a BRUKER minispec mq-ProFiler with a single-sided magnet that generates a static magnetic field of 0.35 T. Therefore, ¹H resonance frequency was equal to 15 MHz. The single-sided NMR was equipped with an RF probe for performing experiments by collecting NMR signal from a sample volume defined from the sample surface to 2 mm inside the sample itself (Stagno et al. 2021b). Hard radiofrequency pulses of duration equal to 6 μs and a dead time acquisition of 2 μs were used. The longitudinal relaxation time (T_1) was acquired by using a Saturation Recovery (SR) sequence with minimum/maximum variable delay time (t) = 1/800 ms, with a repetition time (TR) = 0.02 s, number of averaged scans, NSA = 1024, increment factor 1.2. For each sample, the SR experiment was repeated five times to test the reproducibility of the T_1 measurement and calculate the standard error (STE) associated with the T_1 mean values. On the base of the measured T_1, the TR was set for the transversal relaxation time (T_2) measurement, performed using a Carr-Purcell-Meiboom-Gill (CPMG) sequence. The CPMG was carried out by selecting a delays list from 0.042 ms to 21 ms, with TR = 500 ms, 500 echoes, NSA = 1024, and echo time, TE = 42 μs. This TE allowed of eliminating the contribution of solid wood (i.e. the contribution from immobile protons of the wood polymers, Casieri et al. 2004), which was estimated to be less than 30 μs (Araujo et al. 1992; Hartley et al. 1996), in the T_2 measurements. Also in this case the experiment was repeated five times for each wood sample to extrapolate STE of the T_2 mean values.

Data processing

To obtain the T_1 values, a bi-exponential function:

$$S(t) = M_{1,1} \times \left[1 - \exp\left(-\frac{t}{T_{1,1}} \right) \right] + M_{1,2} \times \left[1 - exp\left(\frac{t}{T_{1,2}} \right) \right]$$

(1)

was fitted to experimental data. In Eq. 1, $T_{1,1}$ and $T_{1,2}$ are the spin–lattice relaxation times belonging to two different water compartments associated with the magnetizations $M_{1,1}$ and $M_{1,2}$ respectively; S(t) is the NMR signal.

Similarly, to quantify T_2 values, a bi-exponential function

$$S(TE) = M_{2,1} \times \exp\left(-\frac{TE}{T_{2,1}}\right) + M_{2,2} \times \exp\left(-\frac{TE}{T_{2,2}}\right) + c$$

(2)

was fitted to the CPMG signal S(TE). $T_{2,1}$ and $T_{2,2}$ are the spin–spin relaxation time components with $M_{2,1}$ and $M_{2,2}$ the associated magnetizations and c a constant to consider the noise floor.

All data were elaborated by using OriginPro 8.5 software. The goodness of each fit was evaluated by using the $\overline{R^2}$ (i.e. the R^2 corrected for the number of the regressors). As an example one T_1 and one T_2 fit for one softwood and one hardwood sample are shown in Fig. 2.

Each T_1 and T_2 component, as well as the associated magnetizations, measured at 46, 78, and 94% RH were plotted as a function of the relative humidity. Then, the k-means clustering algorithm of Matlab2021a (Statistics and Machine Learning Toolbox), which computes the sum of absolute differences i.e. each centroid is the component-wise median of the points in that cluster, was performed to verify the existence of at least two clusters of T_1 and T_2 at RH = 94% among the fifteen samples. Furthermore, correlation plots among wood samples density and all measured relaxation components were obtained.
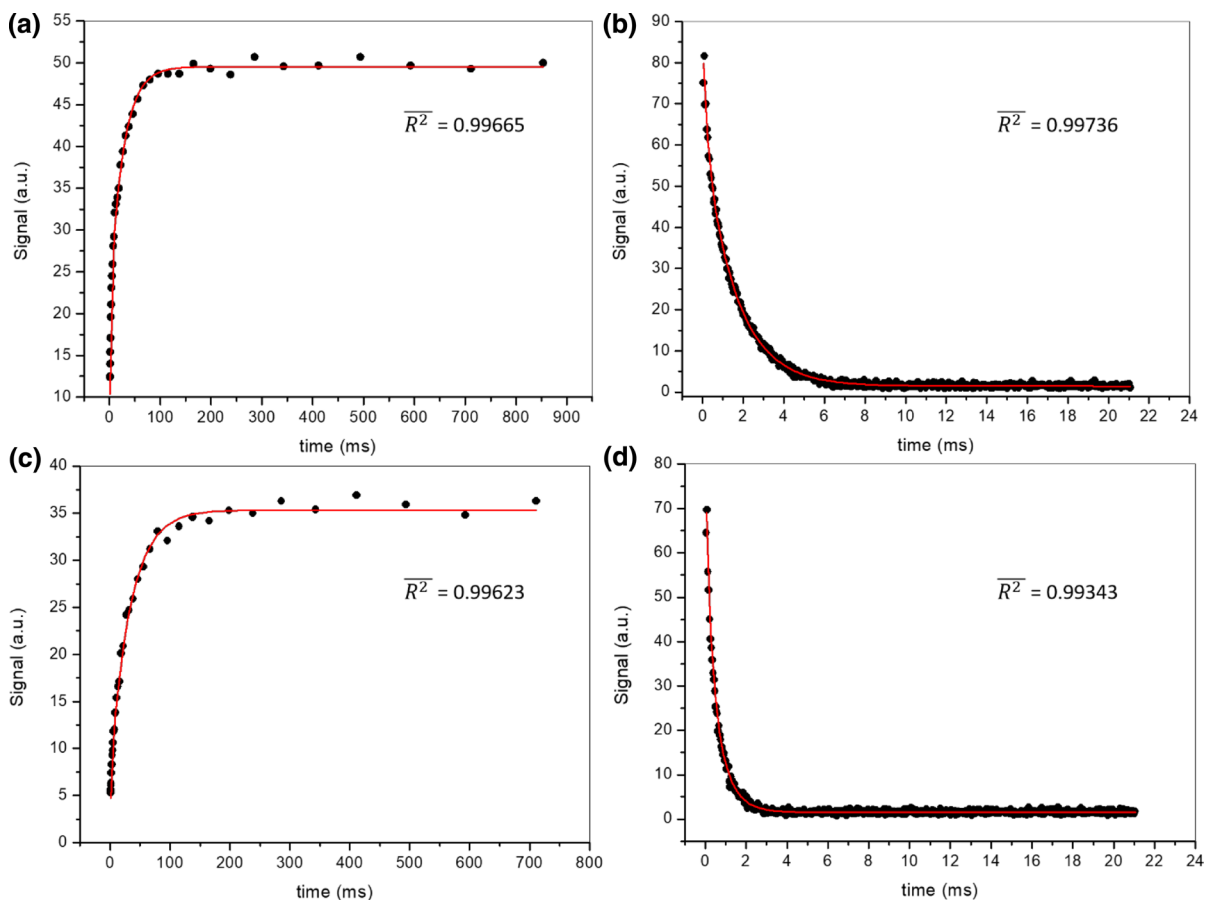

Fig. 2 Example of the bi-exponential fits obtained for T_1 and T_2 data from (**a**, **b**) one hardwood sample (African walnut) and from (**c**, **d**) one softwood sample (red spruce). The $\overline{R^2}$ values used to evaluate the fit goodness are reported

Results

In Table 1 dry density and the EMC calculated at 94% of RH for all the fifteen woods are reported. For the four chosen wood samples (Russian silver fir, European Virginia pine, akatio walnut, and white poplar), T_1 and T_2 components obtained by Eqs. (1) and (2), respectively, are shown in Table 2. The magnetization values $M_{1,1}$, $M_{1,2}$, $M_{2,1}$, $M_{2,2}$, associated with $T_{1,1}$, $T_{1,2}$, $T_{2,1}$ and $T_{2,2}$, respectively, are reported in Table 3. Each relaxation component and magnetization value was then plotted as a function of the relative humidity as displayed in Figs. 3, 4, 5 and 6.

Table 4 shows the longitudinal relaxation times along with the associated magnetizations of all the fifteen samples obtained by the bi-exponential function of Eq. (1). In Table 5 the transversal relaxation times and associated magnetizations obtained by Eq. (2) are displayed. Figure 7 shows the correlation plots among density and relaxation times. The cluster plots that were obtained by correlating the $T_{1,1}$ vs. $T_{2,2}$ (Fig. 8a) and $T_{1,2}$ vs. $T_{2,1}$ (Fig. 8b) and by supposing the existence of two clusters in the k-means algorithm is shown in Fig. 8. Moreover, in Fig. 9 a similar cluster plot but with three hypothesized clusters is shown.

Table 3 Magnetization components and their standard errors (STE) calculated at RH = 46, 78 and 94% by using Eq. (1) and Eq. (2)

	$M_{1,1}$ (%)	$M_{1,2}$ (%)	$M_{2,1}$ (%)	$M_{2,2}$ (%)
46% RH				
Russian silver fir	28 ± 3	72 ± 3	65 ± 4	35 ± 4
European Virginia pine	33 ± 3	66 ± 3	73 ± 2	27 ± 2
Akatio walnut	25 ± 1	75 ± 1	67 ± 2	33 ± 2
White poplar	26 ± 1	74 ± 1	63 ± 2	37 ± 2
78% RH				
Russian silver fir	50 ± 1	50 ± 1	44 ± 5	56 ± 5
European Virginia pine	53 ± 6	47 ± 6	44 ± 3	56 ± 3
Akatio walnut	47 ± 3	53 ± 3	44 ± 2	56 ± 2
White poplar	46 ± 1	54 ± 1	47 ± 1	53 ± 1
94% RH				
Russian silver fir	51 ± 1	49 ± 1	31 ± 4	69 ± 4
European Virginia pine	54 ± 4	46 ± 4	38 ± 4	62 ± 4
Akatio walnut	45 ± 1	55 ± 1	24 ± 1	76 ± 1
White poplar	39 ± 1	61 ± 1	35 ± 1	65 ± 1

Discussion

This work aimed to discriminate among different wood samples on the base of the NMR relaxation of their cell wall water in the hygroscopic range. To develop a non-invasive NMR protocol for in situ

Table 2 T_1 and T_2 components and their standard errors (STE) calculated at RH = 46, 78, 94% by using Eq. (1) and Eq. (2)

	$T_{1,1}$ (ms)	$T_{1,2}$ (ms)	$T_{2,1}$ (ms)	$T_{2,2}$ (ms)
46% RH				
Russian silver fir	0.89 ± 0.19	61.51 ± 4.78	0.16 ± 0.01	0.57 ± 0.01
European Virginia pine	1.13 ± 0.09	54.32 ± 4.10	0.152 ± 0.002	0.53 ± 0.01
Akatio walnut	1.19 ± 0.05	59.02 ± 2.23	0.152 ± 0.004	0.57 ± 0.02
White poplar	1.34 ± 0.08	66.99 ± 2.09	0.152 ± 0.004	0.550 ± 0.004
78% RH				
Russian silver fir	0.84 ± 0.05	46.91 ± 2.50	0.17 ± 0.01	0.60 ± 0.01
European Virginia pine	1.01 ± 0.09	36.65 ± 1.80	0.180 ± 0.004	0.60 ± 0.01
Akatio walnut	1.62 ± 0.06	44.34 ± 1.95	0.178 ± 0.004	0.87 ± 0.01
White poplar	1.89 ± 0.04	52.00 ± 1.83	0.178 ± 0.004	0.98 ± 0.01
94% RH				
Russian silver fir	1.44 ± 0.05	36.51 ± 1.48	0.178 ± 0.004	0.69 ± 0.01
European Virginia pine	1.39 ± 0.12	28.24 ± 1.97	0.20 ± 0.01	0.70 ± 0.01
Akatio walnut	1.67 ± 0.04	30.33 ± 0.64	0.248 ± 0.004	1.33 ± 0.01
White poplar	2.05 ± 0.11	39.49 ± 1.71	0.192 ± 0.004	1.38 ± 0.02

Fig. 3 **a** Plot of $T_{1,1}$ as a function of RH and **b** plot of $T_{1,2}$ as a function of RH for two softwoods (Russian silver fir and European Virginia pine) and for two hardwoods (white poplar and akatio walnut). Lines are for illustration purposes only


(a)

(b)
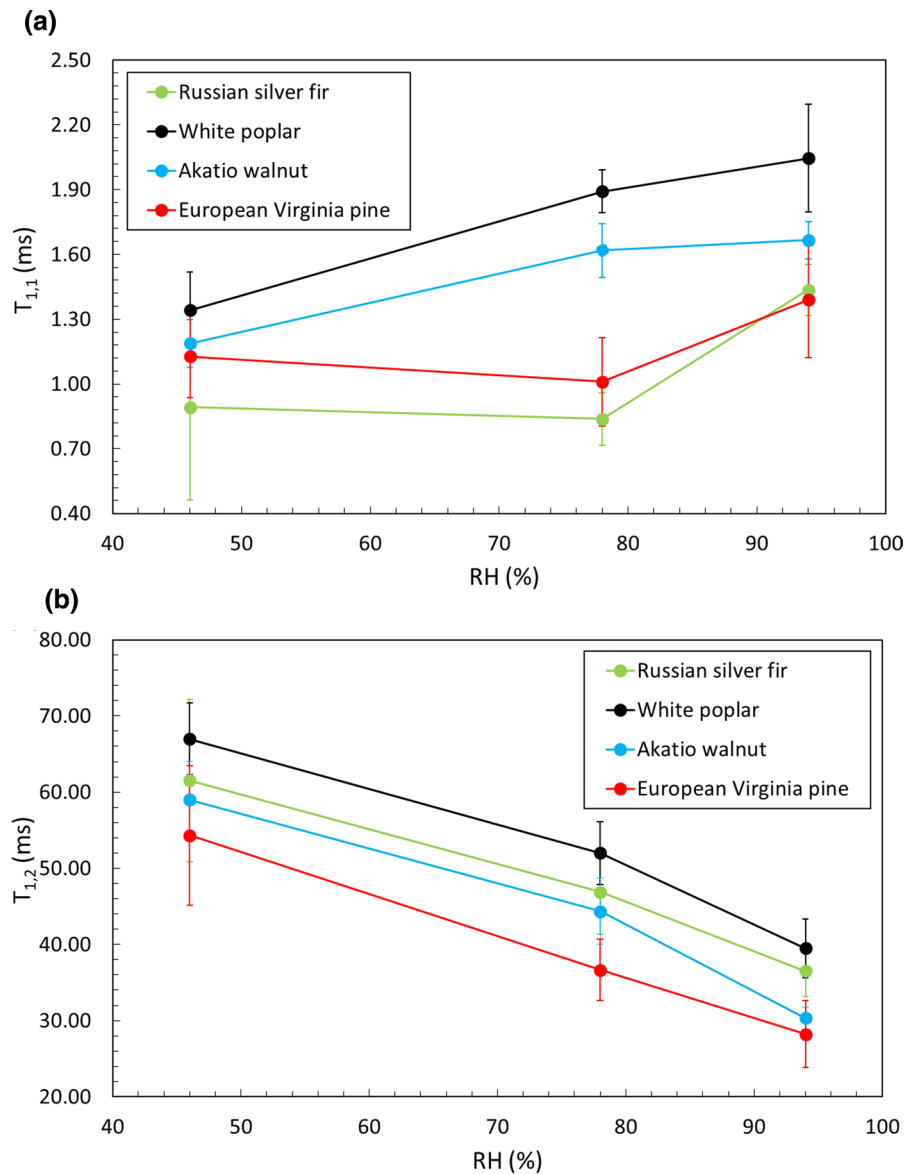
investigation useful in the wood industry and/or for the applications on high-humidity and waterlogged cultural heritage objects, a portable NMR instrument was used. In the following, to better deal with and discuss the various observations and results obtained, the discussion section was divided into several paragraphs.

NMR relaxation times components assignment and their dependence on RH

A different behavior of the two components of T_1 relaxation and the two components of T_2 relaxation is highlighted in Figs. 3 and 4. Considering the longitudinal relaxation time, some authors (Fantazzini et al. 2006; Bonnet et al. 2017; Rostom et al. 2020) pointed out the existence of two different components below the FSP. A fast T_1 component of a few ms or hundreds of μs, which is due to water bound to the cell walls, and a slow T_1 of tens of ms, which is associated with

Fig. 4 a Plot of $T_{2,1}$ as a function of RH and **b** plot of $T_{2,2}$ as a function of RH for two softwoods (Russian silver fir and European Virginia pine) and for two hardwoods (white poplar and akatio walnut). Lines are for illustration purposes only
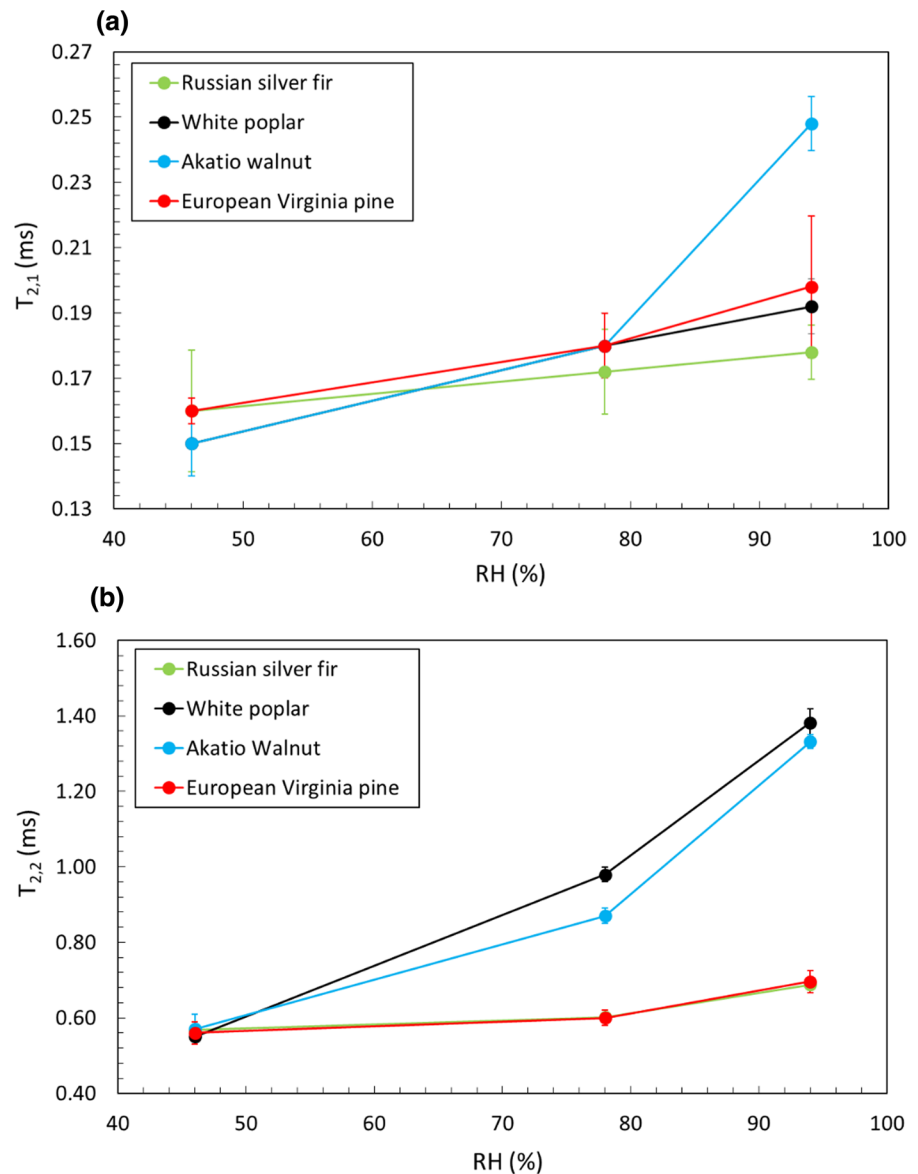

the water protons of wood polymers. In this regard, the component $T_{1,1}$ displayed in Fig. 3a, which is of the order of few ms, can be attributed to bound water in the cell walls while the second component $T_{1,2}$ (Fig. 3b), much greater and around tens of ms, can be associated with relatively immobile water within the wood polymers.

Regarding the transversal relaxation time, previous works (Araujo et al. 1992; Hartley et al. 1992; Labbé et al. 2002; Thygesen and Elder 2009) identified a T_2 component around 0.2–3 ms increasing with RH as bound water. Therefore, we can associate the fast

component $T_{2,1}$ (Fig. 4a) with water protons tightly bound to macromolecules and the slow component $T_{2,2}$ (Fig. 4b) with protons of cell wall-bound water (Casieri et al. 2004; Thygesen and Elder 2009). On the other hand, as the investigated wood samples were below the fiber saturation point, we did not detect the lumen water that is characterized by T_2 around tens of milliseconds (Labbé et al. 2002). Moreover, because we used a TE = 0.04 ms in the CPMG experiments, we did not measure the faster T_2 component belonging to solid wood (Casieri et al. 2004), estimated to be around 0.01 ms by Labbè et al. (Labbé et al. 2002).

Fig. 5 a Plot of $M_{1,1}$ as a function of RH and **b** plot of $M_{1,2}$ as a function of RH for two softwoods (Russian silver fir and European Virginia pine) and for two hardwoods (white poplar and akatio walnut). Lines are for illustration purposes only
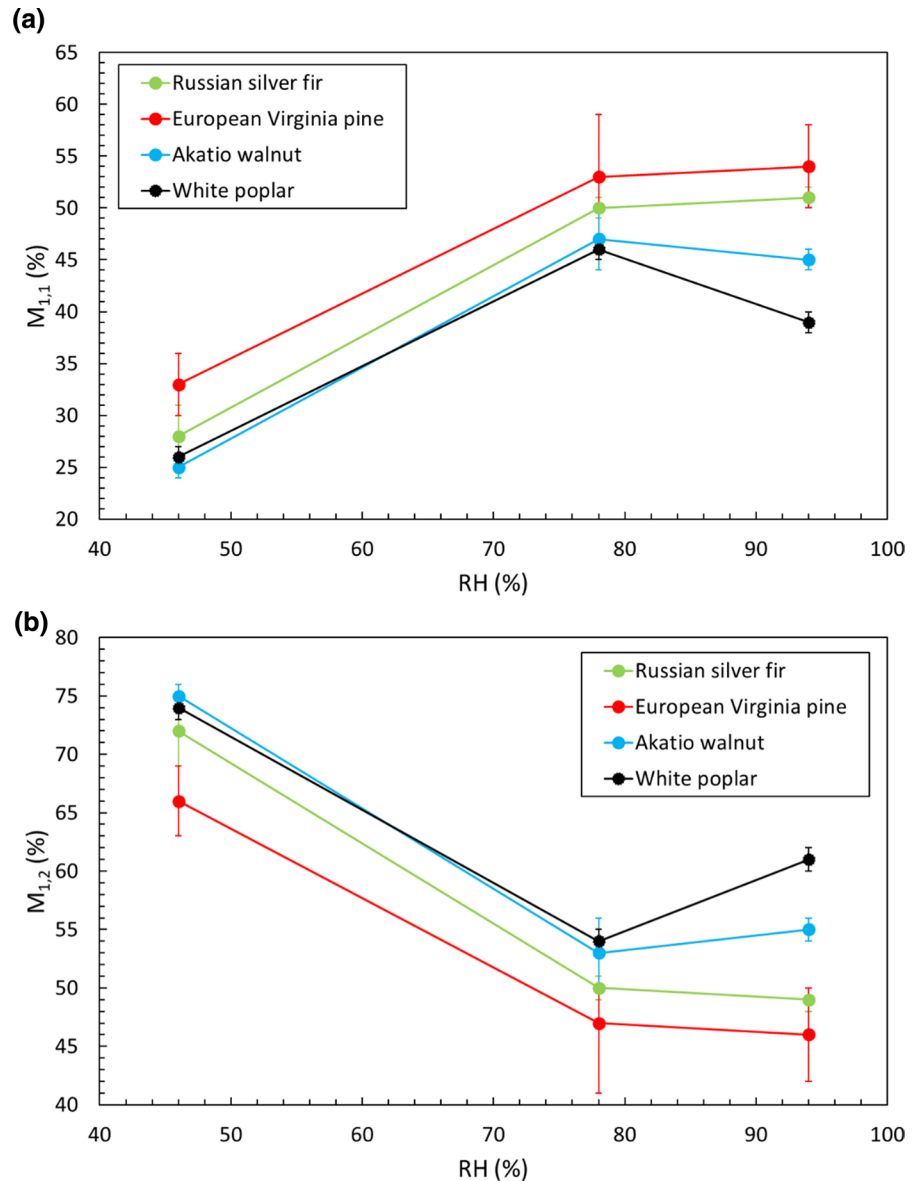

Cell walls reservoir

In Fig. 3, the effect of RH increase on the T_1 associated with the cell walls ($T_{1,1}$) is visible for all four wood samples. Particularly, this component (Fig. 3a), ranging from a minimum of 0.8 ms to a maximum of 2 ms, shows a quite different behavior among softwoods and hardwoods. For the two hardwoods, white poplar and akatio walnut, the $T_{1,1}$ appears to increase with the RH increment. This is due to the growing hydration of the wood cell walls which determines a slower longitudinal relaxation time. In particular, the

$T_{1,1}$ increment is higher when RH increases from 46 to 78% while it is lower from RH = 78% to 94%. The trend of the $T_{1,1}$ of the two hardwoods seems to indicate that we are close to a saturation process that can be identified as the fiber saturation point.

In the two softwoods, Russian silver fir and European Virginia pine, the $T_{1,1}$ seems to be constant when RH changes from 46 to 78% and it starts to increase rapidly when RH grows from 78 to 94% reaching a lower maximum value compared to that of the hardwoods. This result can be explained by the fact that the hardwood samples catch more water

Fig. 6 **a** Plot of $T_{2,1}$ as a function of RH and **b** plot of $T_{2,2}$ as a function of RH for two softwoods (Russian silver fir and European Virginia pine) and for two hardwoods (white poplar and akatio walnut). Lines are for illustration purposes only
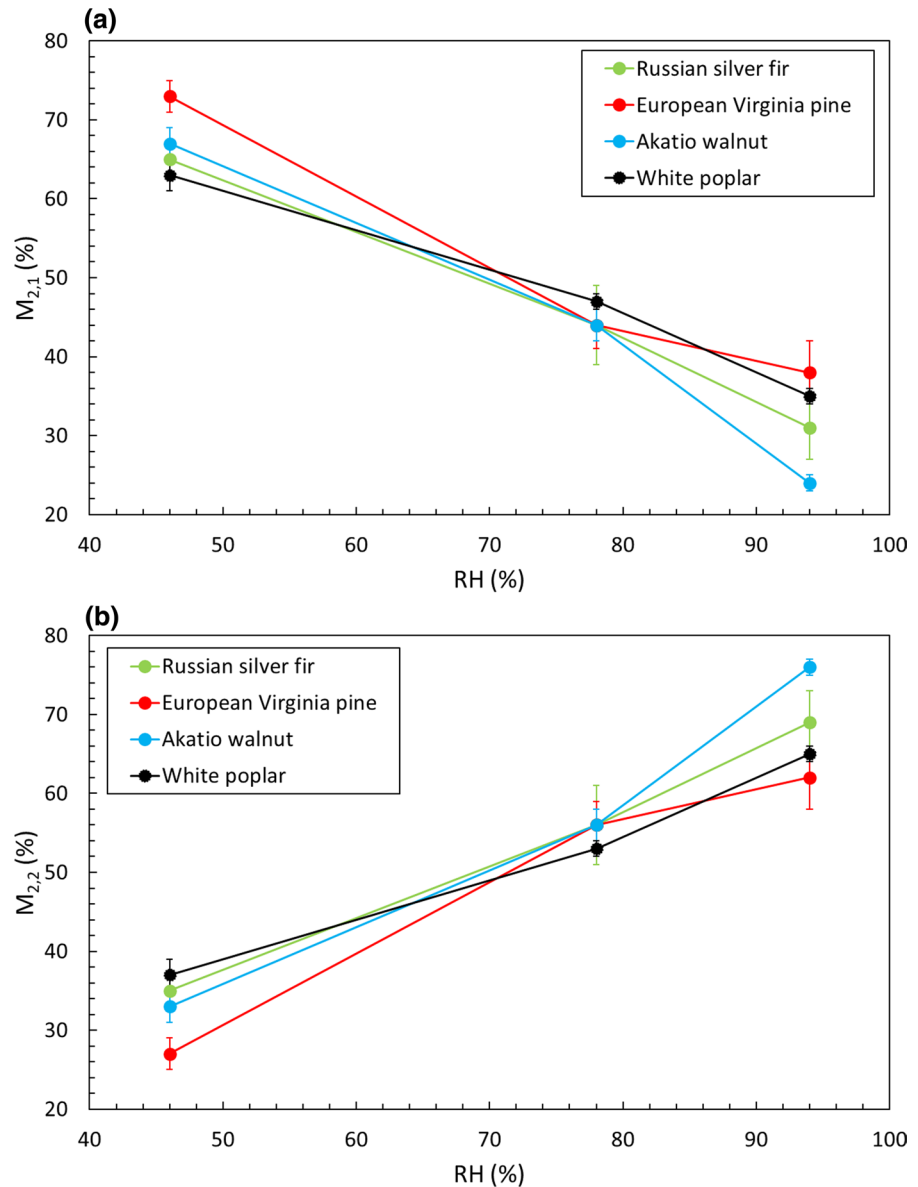
molecules thanks to their higher hemicellulose content compared to the softwood samples. Also in the softwoods, the $T_{1,1}$ increment is associated with the growing hydration of the cell walls, but this seems to be gained drastically for RH > 78%. This behavior may be a consequence of the hemicellulose softening that at room temperature (T = 20 °C) occurs around RH = 75% (Olsson and Salmén 2004; Engelund et al. 2013).

The $T_{2,2}$ component of wood cell walls (Fig. 4b), grows from 0.53 to 1.38 ms describing progressive

hydration of the wood cell walls mainly ascribable to hemicelluloses softening. Its growth is faster above RH = 78% due to the glass transition of hemicelluloses as described by Engelund et al. (Engelund et al. 2013). This T_2 component also shows a distinct behavior among softwoods and hardwoods reflecting their different hygroscopicity. On this subject, hardwoods have cell walls made by a higher amount of hemicellulose (Holtzapple 2003) that is characterized by a lot of polar groups (OH groups)

Table 4 T_1 components calculated by Eq. (1) and their standard errors (STE), along with the magnetization values, at RH = 94% for the fifteen samples

Common name	$T_{1,1} \pm$ STE (ms)	$M_{1,1}$ (%)	$T_{1,2} \pm$ STE (ms)	$M_{1,2}$ (%)
bahia walnut	1.39 ± 0.08	46	26.76 ± 1.37	54
white poplar	2.05 ± 0.11	39	39.49 ± 1.71	61
red spruce	1.26 ± 0.12	19	33.09 ± 0.61	81
Russian silver fir	1.44 ± 0.05	51	36.51 ± 1.48	49
akatio walnut	1.67 ± 0.04	45	30.33 ± 0.64	55
European silver fir	1.19 ± 0.03	59	23.64 ± 0.76	41
sessile oak	1.69 ± 0.19	8	67.66 ± 0.59	92
English walnut	2.55 ± 0.06	8	84.58 ± 1.70	92
tanganyika walnut	1.66 ± 0.06	49	39.44 ± 1.13	51
sapele mahogany	1.50 ± 0.4	8	81.13 ± 2.33	92
Australian red cedar	1.67 ± 0.23	12	59.85 ± 1.48	88
European Virginia pine	1.39 ± 0.12	54	28.24 ± 1.97	46
African walnut	1.92 ± 0.08	44	28.38 ± 0.87	56
American red spruce	1.15 ± 0.17	17	33.76 ± 0.58	83
American Virginia pine	1.04 ± 0.03	56	22.80 ± 0.59	44

Table 5 T_2 components calculated by Eq. (2) and their standard errors (STE), along with the magnetization values, at RH = 94% for the fifteen samples

Common name	$T_{2,1} \pm$ STE (ms)	$M_{2,1}$ (%)	$T_{2,2} \pm$ STE (ms)	$M_{2,2}$ (%)
bahia walnut	0.214 ± 0.004	35	1.098 ± 0.004	65
white poplar	0.192 ± 0.004	35	1.38 ± 0.02	65
red spruce	0.19 ± 0.01	32	0.64 ± 0.01	68
Russian silver fir	0.178 ± 0.004	31	0.69 ± 0.01	69
akatio walnut	0.24 ± 0.01	24	1.33 ± 0.01	76
European silver fir	0.196 ± 0.004	28	0.806 ± 0.004	72
sessile oak	0.280 ± 0.004	17	0.952 ± 0.004	83
English walnut	0.216 ± 0.004	32	1.25 ± 0.01	68
tanganyika walnut	0.190 ± 0.004	41	1.096 ± 0.004	59
sapele mahogany	0.238 ± 0.002	31	1.546 ± 0.004	69
Australian red cedar	0.22 ± 0.01	25	0.90 ± 0.02	75
European Virginia pine	0.20 ± 0.01	38	0.70 ± 0.01	62
African walnut	0.25 ± 0.01	28	1.606 ± 0.004	72
American red spruce	0.214 ± 0.004	32	0.72 ± 0.01	68
American Virginia pine	0.192 ± 0.004	35	0.636 ± 0.004	65

able to retain water increasing wood hygroscopicity (García Esteban et al. 2005).

4.1.3 Polymers water reservoir. The $T_{1,2}$ component in Fig. 3b shows an opposite behavior as a function of RH compared to that of the $T_{1,1}$ (Fig. 3a). Starting from a value of 50–60 ms at RH = 46%, the $T_{1,2}$ decreases for both softwoods and hardwoods with the increase of RH, reaching a minimum value around 30–40 ms. This is explainable considering that water tightly bound to polymers gains mobility with the RH increment. In the solid-like range, this

increase of mobility is associated with a speeding up of the spin–lattice relaxation time due to the faster exchange of energy between spins and lattice (Brown and Koenig 1992).

In this regard, the $T_{2,1}$ component (Fig. 4a) spanning from 0.15 to 0.24 ms, appears to slightly grow during the RH increment except for akatio walnut that shows a rapid increase (from 0.18 to 0.25 ms) when RH changes from 78 to 94%. This observation can indicate a greater mobility of water protons in akatio walnut macromolecules and that it
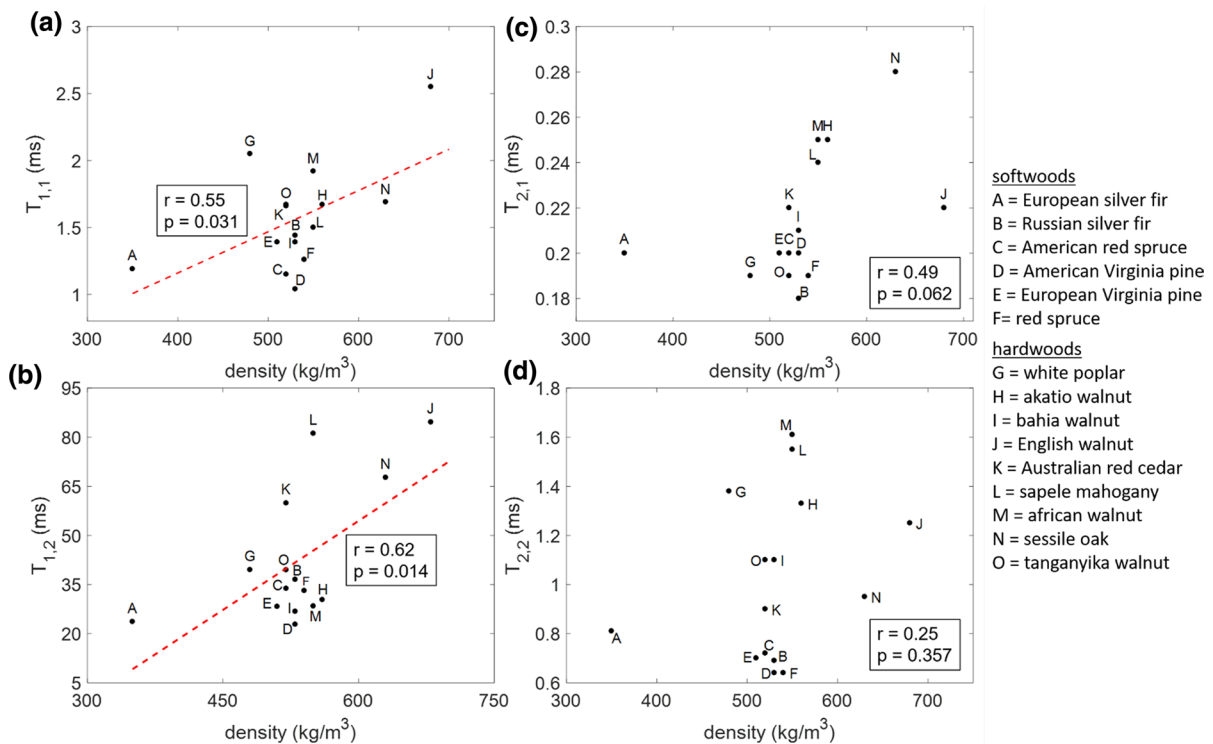
Fig. 7 Correlation plots among wood density and relaxation times components of the cell wall reservoir, (**a**) and (**d**), and of the polymers water reservoir, (**b**) and (**c**), at RH=94%. The displayed parameters r and p indicate the correlation coefficient and the p-value, respectively. The dashed red line indicates the significant linear correlation

is approaching the FSP. In fact, as described in the literature (Jankowska and Kozakiewicz 2016), the FSP is negatively correlated with the wood density so denser woods have a lower FSP. The akatio walnut sample investigated in this paper has the highest density (around 560 kg/m^3, see Table 1) among the other three samples and for this reason, a low FSP is expected. In general, the $T_{2,1}$ component is quite similar for softwoods and hardwoods and it describes the slow variation of mobility of the water protons tightly bound to macromolecules.

Magnetization dependence on RH

As shown in Fig. 5 and Fig. 6, the magnetization values associated with the T_1 and T_2 components change by varying the RH. For the magnetizations associated with the $T_{1,1}$ and $T_{2,2}$ components (Fig. 5a and Fig. 6b), which describe the cell walls reservoir, it is possible to notice an increase with the RH rise. This increase is quite linear for $M_{2,2}$, whereas for $M_{1,1}$

there is a quick increment only until 78%. Despite $M_{1,1}$ and $M_{2,2}$ values remain quite similar for softwoods and hardwoods, after RH=78% the $M_{1,1}$ seems to reach a plateau for the two softwoods (Russian silver and European Virginia pine), whereas for the two hardwoods (akatio walnut and white poplar) it weakly decreases. The increase of $M_{1,1}$ and $M_{2,2}$ indicates that the number of protons in the cell walls reservoir grows with the RH increase.

An opposite behaviour can be seen for the magnetizations $M_{1,2}$ and $M_{2,1}$, which are associated with $T_{1,2}$ and $T_{2,1}$ of the polymers water reservoir. $M_{1,2}$ and $M_{2,1}$ decrease with the RH increase. Also in this case the decrease is fast and quite linear with the RH increase for $M_{2,1}$, while it is slow for $M_{1,2}$ after RH=78%. For both the two hardwoods (akatio walnut and white poplar), $M_{1,2}$ seems to increase by passing from RH=78 to 94%.

The behaviour observed between RH=78 and 94% for the magnetization associated with the relaxation

Fig. 8 Cluster plots obtained by k-means algorithm between $T_{1,1}$ and $T_{2,2}$ (**a**) and $T_{1,2}$ and $T_{2,1}$ (**b**) of the fifteen samples at RH = 94%. In **a** the centroid of cluster 1 is [74.39, 0.23] and of cluster 2 is [30.33, 0.20]. In **b** softwoods cluster has centroid of [1.22, 0.69] and hardwoods cluster of [1.67, 1.25]
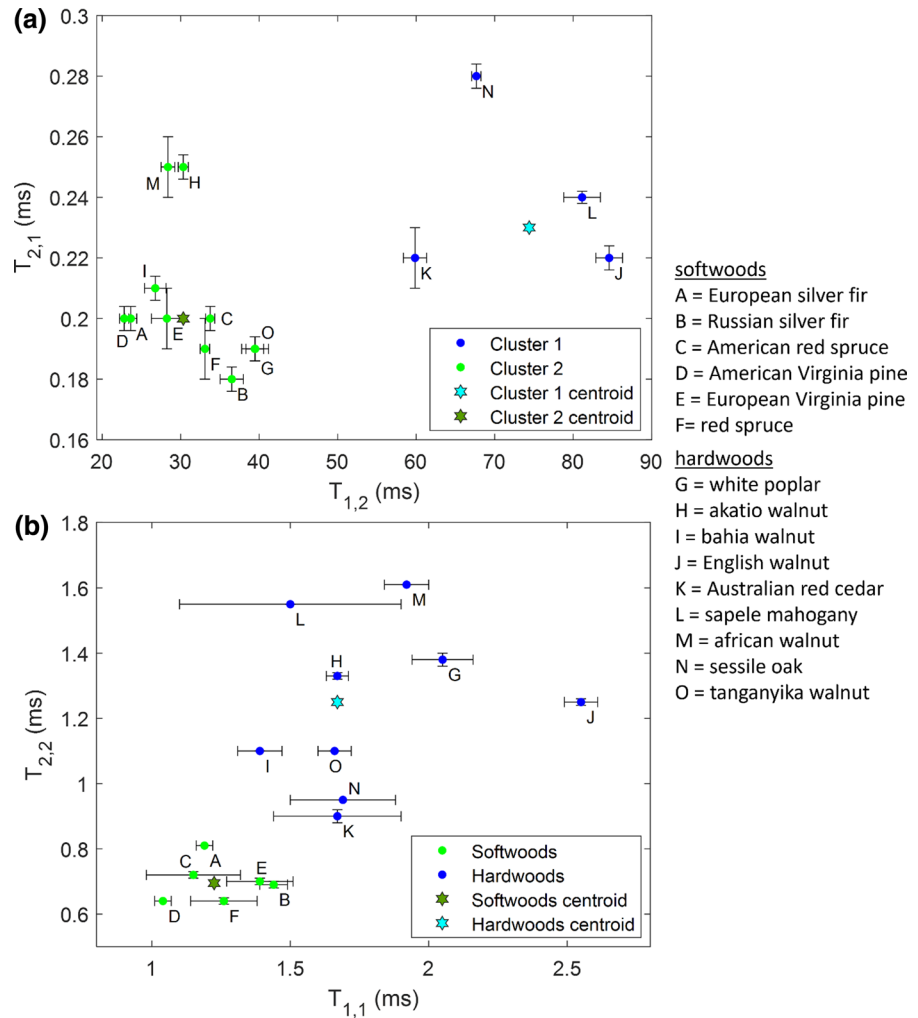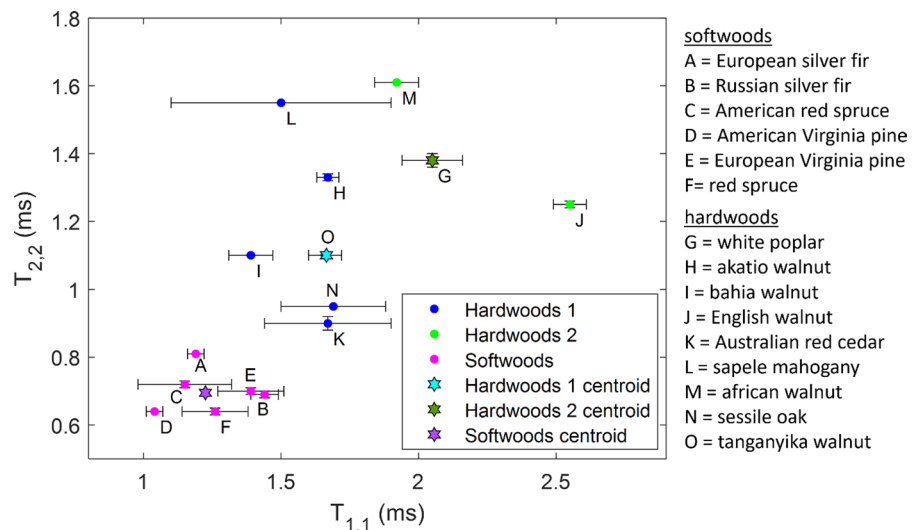

Fig. 9 Cluster plot obtained by hypothesizing three clusters in k-means algorithm between $T_{1,1}$ and $T_{2,2}$ of the fifteen samples at RH = 94%. For the cluster of hardwoods 1 the centroid is [1.66, 1.10], for hardwoods 2 is [2.05, 1.38], whereas for softwoods is [1.22, 0.69]

time T_1 of the two hardwoods may indicate that the fiber saturation point is approaching.

Relaxation times vs. density correlation of the fifteen woods at RH = 94%

As expected, the plot in Fig. 7 suggests that T_1 moderately correlates with the wood dry density (kg/m³), as previously shown by Stagno et al. (2020). The dependence of $T_{1,1}$ and $T_{1,2}$ on the dry density of woods indicates that T_1 is also affected by intrinsic features of the wood. Particularly, English walnut is characterized by the longest T_1 and the highest dry density associated with its compact structure due to a diffuse-porous ring with infrequent pores and frequent tyloses (Thygesen and Elder 2009). Conversely, European silver fir has the lowest density and the shortest T_1 because of its homogeneous structure constituted by about 95% of open elements, i.e. tracheids (Araujo et al. 1992; Thygesen et al. 2010).

Clustering

In Sects. 4.1 and 4.2 the dependence of the relaxation times and magnetizations on RH for two softwoods and two hardwoods has been discussed. By varying the RH, we observed a significant difference in the behavior of the relaxation times of the two softwoods compared to those of the two hardwoods, whereas the magnetization values seem to be quite similar for both softwood and hardwood. For this reason, in the following sub-sections we discussed the possibility of using the relaxation times rather than the magnetizations in the cluster analysis for differentiating among softwoods and hardwoods.

4.4.1 Two clusters hypothesis. The main purpose of clustering by hypothesizing two clusters was to detect a possible different behavior among softwoods and hardwoods based on the measured relaxation times. The plot in Fig. 8a shows how the different species of wood are distributed according to their $T_{1,1}$ and $T_{2,2}$ relaxation times. A clear differentiation of the cell wall reservoir between softwoods and hardwoods is visible. Softwoods cluster centroid is [1.22, 0.69], which indicates that softwood samples are distributed around the median value of $T_{1,1} = 1.22$ ms and of $T_{2,2} = 0.69$ ms. Indeed, while hardwoods seem to be spread among different values of T_1, softwoods occupy a quite narrow region of the plot that roughly

ranges from 1 to 1.5 ms. Moreover, the hardwoods cluster centroid is [1.67, 1.25]. Indeed, hardwoods show higher values of $T_{2,2}$ if compared to softwoods. Indeed, softwoods have $T_{2,2}$ always shorter than 0.806 ± 0.004 ms, and hardwoods always longer than 0.90 ± 0.02 ms. On average, at RH = 94% the cell wall reservoir of softwoods is characterized by lower values of T_1 and T_2 than the cell wall reservoir of hardwoods.

In Fig. 8b, a similar result is shown but considering the $T_{1,2}$ and $T_{2,1}$ components. Two different clusters can be observed: cluster 1 with a centroid of [74.39, 0.23] and cluster 2 with a centroid of [30.33, 0.20]. As for the plot in Fig. 8a, the $T_{1,2}$ component of hardwoods is spread to different values. On contrary, softwoods show shorter $T_{1,2}$. The $T_{2,1}$ component is quite similar for all the woods. This result suggests that on the base of the polymers water reservoir it is not possible to distinguish among softwood and hardwood samples because of their quite similar T_1 and T_2 relaxation times. Anyway, two clusters were detected with cluster 1 that contains four hardwoods (sessile oak, sapele mahogany, English walnut, and Australian red cedar) characterized by long $T_{1,2}$ and $T_{2,1}$ that may indicates a greater mobility of their polymers water reservoir.

4.4.2 Three clusters hypothesis. In this work we tried to explore the potential of portable NMR in differentiating among woods with different characteristics. To this end, we also evaluated the existence of other possible clusters by using the $T_{1,1}$ and $T_{2,2}$ components, which are the relaxation times that provided a good differentiation among softwoods and hardwoods. A three clusters analysis was performed and shown in Fig. 9. This plot suggests two sub-clusters of the hardwoods cluster. The cluster called hardwoods 2, with centroid [2.05, 1.38], contains the samples with longer $T_{1,1}$ (English walnut, white poplar, and African walnut), whereas the cluster called hardwoods 1, with centroid [1.66, 1.10], the samples with shorter $T_{1,1}$ (sapele mahogany, akatio walnut, bahia walnut, sessile oak, tanganyika walnut, and Australian red cedar). Because the two sub-clusters of hardwoods are separated only on the base of the $T_{1,1}$ component that for some samples is affected by a quite high error, we suggest taking with care the result shown in the three clusters plot of Fig. 9.
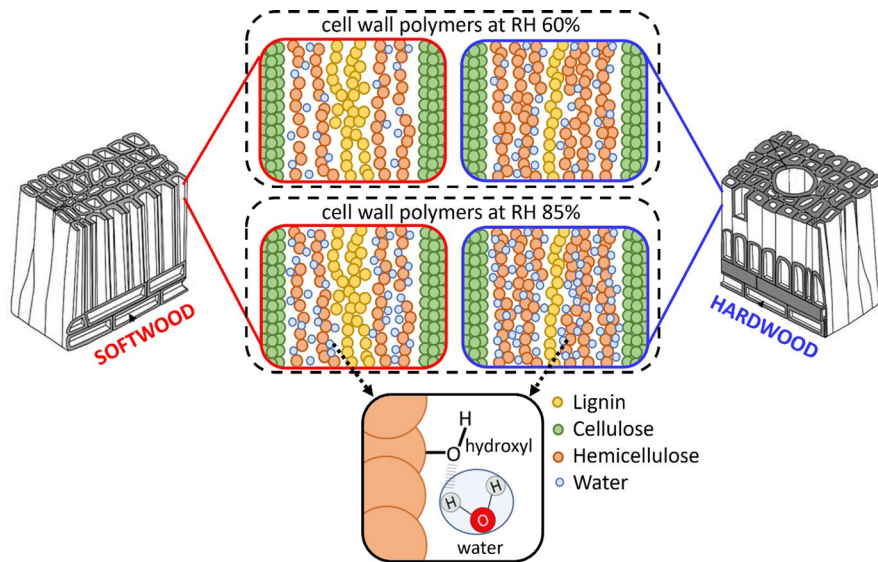
Fig. 10 Schematic representation of cell wall polymers hydration in parallel with the RH increase. Hydroxyl groups of hemicellulose catch water molecules through hydrogen bonds. The $T_{1,1}$ and $T_{2,2}$ relaxation components measured in this work and associated with the cell wall-bound water can be considered as markers allowing to discriminate between softwood and hardwood on the base of their different hygroscopic behavior mainly due to their different hemicellulose amount. Hardwoods are characterized by a greater number of hemicellulose macromolecules that capture more water molecules during hydration. Therefore, on average, they show higher $T_{1,1}$ and $T_{2,2}$ than softwoods

Final discussion

In Fig. 10 a schematic representation of the hygroscopic behavior of the wood cell wall polymers exploited in this work to discriminate between softwood and hardwood is displayed. Specifically, in parallel with the increase of RH, the hemicellulose hydrates more. The hydroxyl groups of the hemicellulose capture water molecules through hydrogen bonds that affect the NMR relaxation times of the cell wall reservoir ($T_{1,1}$ and $T_{2,2}$), which allow discrimination between softwood and hardwood. Hardwoods have a higher hemicellulose content compared to softwoods; therefore their cell walls can reach greater hydration with more mobile water molecules that are bound to the hemicellulose hydroxyls.

Conclusions

In this work, we tested the hypothesis of discriminating among softwoods and hardwoods of different botanical species based on their NMR relaxation times. To this end, a non-invasive protocol was tested on fifteen softwood and hardwood samples below the fiber saturation point by using a portable low-field NMR instrument. The results obtained in this paper suggest that, to discriminate between different softwoods and hardwoods by NMR relaxation times, it is necessary to perform the NMR measurements below the FSP but at relative humidity higher than 75% that corresponds to the humidity at which the hemicellulose softening occurs at room temperature. Moreover, both the transversal and longitudinal relaxation times of the cell walls bound water ($T_{1,1}$ and $T_{2,2}$) and polymers water reservoirs ($T_{1,2}$ and $T_{2,1}$) can be quantified. On average, the NMR relaxation times associated with the cell walls water reservoir allow to discriminate among hardwoods and softwoods and between two sub-clusters of hardwoods. Specifically, the $T_{2,2}$ is the marker parameter that better discriminates between softwoods group and hardwoods group because it exhibits a significant variation among softwoods and hardwoods. Furthermore, according to results obtained below the FSP, small RH variations might affect the relaxation times. A controlled environment with constant relative humidity and temperature is therefore highly recommended to

perform non-biased NMR relaxation time measurement. The NMR protocol presented in this study can be enhanced by studying a greater number of wood species and including further NMR parameters, such as the water diffusion coefficient (Stagno et al. 2021a, 2021c), which may reflect the different hygroscopic behavior of softwood and hardwood connected to the different ultrastructural composition of their cell walls.

In conclusion, although limited to only 15 botanical species, the non-invasive NMR protocol performed by a portable instrument, allowed a preliminary discrimination among species of softwood and hardwood, which could be useful for the wood industry and/or for the applications on high-humidity and waterlogged cultural heritage objects.

Declaration

References

Alesiani M, Proietti F, Capuani S, Paci M, Fioravanti M, Maraviglia B (2005) 13C CPMAS NMR spectroscopic analysis applied to wood characterization. Appl Magn Reson. https://doi.org/10.1007/BF03167005

Almeida G, Gagné S, Hernández RE (2007) A NMR study of water distribution in hardwoods at several equilibrium moisture contents. Wood Sci Technol. https://doi.org/10.1007/s00226-006-0116-3

Araujo CD, MacKay AL, Hailey JRT, Whittall KP, Le H (1992) Proton magnetic resonance techniques for characterization of water in wood: application to white spruce. Wood Sci Technol. https://doi.org/10.1007/BF00194466

Bartolucci B, Frasca F, Siani AM, Bertolin C (2021) Calibration of acoustic emission parameters in relation to the equilibrium moisture content variations in a *Pinus sylvestris* beam. Appl Sci. https://doi.org/10.3390/app11115236

Beckstein O, Sansom MSP (2003) Liquid-vapor oscillations of water in hydrophobic nanopores. Proc Natl Acad Sci U S A. https://doi.org/10.1073/pnas.1136844100

Berry SL, Roderick ML (2005) Plant-water relations and the fibre saturation point. New Phytol 168:25

Bonnet M, Courtier-Murias D, Faure P, Rodts S, Care S (2017) NMR determination of sorption isotherms in earlywood and latewood of Douglas fir. Identification of bound water components related to their local environment. Holzforschung. https://doi.org/10.1515/hf-2016-0152

Brown RD, Koenig SH (1992) 1 /T1p and low-field 1 / T1 of Tissue water protons arise from magnetization transfer to macromolecular solid-state broadened lines. Magn Reson Med. https://doi.org/10.1002/mrm.1910280115

Camuffo D (2018) Standardization activity in the evaluation of moisture content. J Cult Herit. https://doi.org/10.1016/j.culher.2018.03.021

Capuani S, Stagno V, Missori M, Sadori L, Longo S (2020) High-resolution multiparametric MRI of contemporary and waterlogged archaeological wood. Magn Reson Chem. https://doi.org/10.1002/mrc.5034

Casieri C, Senni L, Romagnoli M, Santamaria U, De Luca F (2004) Determination of moisture fraction in wood by mobile NMR device. J Magn Reson. https://doi.org/10.1016/j.jmr.2004.09.014

Chami Khazraji A, Robert S (2013) Self-assembly and intermolecular forces when cellulose and water interact using molecular modeling. J Nanomater. https://doi.org/10.1155/2013/745979

Elder T, Houtman C (2013) Time-domain NMR study of the drying of hemicellulose extracted aspen (*Populus tremuloides* Michx.). Holzforschung. https://doi.org/10.1515/hf-2012-0130

Engelund ET, Thygesen LG, Svensson S, Hill CAS (2013) A critical discussion of the physics of wood-water interactions. Wood Sci Technol. https://doi.org/10.1007/s00226-012-0514-7

European Committee for Standardization (2017) EUROPEAN STANDARD EN 16682 : Conservation of cultural heritage—Methods of measurement of moisture content in materials constituting immovable cultural heritage

Fantazzini P, MacCotta A, Gombia M, Garavaglia C, Brown RJS, Brai M (2006) Solid–liquid nuclear magnetic resonance relaxation and signal amplitude relationships with ranking of seasoned softwoods and hardwoods. J Appl Phys. https://doi.org/10.1063/1.2354322

Fredriksson M, Thygesen LG (2017) The states of water in Norway spruce (*Picea abies* (L.) Karst.) studied by low-field nuclear magnetic resonance (LFNMR) relaxometry: assignment of free-water populations based on quantitative wood anatomy. Holzforschung. https://doi.org/10.1515/hf-2016-0044

García Esteban L, Gril J, Palacios DPD, P, Guindeo Casasús A, (2005) Reduction of wood hygroscopicity and associated dimensional response by repeated humidity cycles. Ann for Sci. https://doi.org/10.1051/forest:2005020

Glass Samuel V, Zelinka SL (2010) Wood handbook, chapter 04: moisture relations and physical properties of wood. Wood Handb wood as an Eng Mater

Hartley ID, Kamke FA, Peemoeller H (1992) Cluster theory for water sorption in wood. Wood Sci Technol. https://doi.org/10.1007/BF00194465

Hartley ID, Avramidis S, MacKay AL (1996) H-NMR studies of water interactions in sitka spruce and western hemlock: moisture content determination and second moments. Wood Sci Technol. https://doi.org/10.1007/BF00224966

Holtzapple MT (2003) Hemicelluloses. In: Encyclopedia of Food Sciences and Nutrition

Jankowska A, Kozakiewicz P (2016) Determination of fibre saturation point of selected tropical wood species using different methods. Drewno. https://doi.org/10.12841/wood.1644-3985.C07.12

Kulasinski K, Guyer R, Derome D, Carmeliet J (2015) Water adsorption in wood microfibril-hemicellulose system: role of the crystalline-amorphous interface. Biomacromology. https://doi.org/10.1021/acs.biomac.5b00878

Labbé N, De Jéso B, Lartigue JC, Daudé G, Pétraud M, Ratier M (2002) Moisture content and extractive materials in maritime pine wood by low field 1H NMR. Holzforschung. https://doi.org/10.1515/HF.2002.005

Labbé N, De Jéso B, Lartigue JC, Daudé G, Pétraud M, Ratier M (2006) Time-domain 1H NMR characterization of the liquid phase in greenwood. Holzforschung. https://doi.org/10.1515/HF.2006.043

Menon RS, MaCkay AL, Hailey JRT, Bloom M, Burgess AE, Swanson JS (1987) An NMR determination of the physiological water distribution in wood during drying. J Appl Polym Sci. https://doi.org/10.1002/app.1987.070330408

Nilsson LO (2018) Methods of measuring moisture in building materials and structures: State-of-the-art report of the rilem technical committee 248-mmb. In: RILEM State-of-the-Art Reports

Noack D (1989) Wood–water relations. Christen Skaar. Q Rev Biol. https://doi.org/10.1086/416506

Olsson AM, Salmén L (2004) The softening behavior of hemicelluloses related to moisture. In: ACS symposium series

Rostom L, Courtier-Murias D, Rodts S, Care S (2020) Investigation of the effect of aging on wood hygroscopicity by 2D 1H NMR relaxometry. Holzforschung. https://doi.org/10.1515/hf-2019-0052

Schirarend C (1986) Siau, J. F., Transport processes in wood. Springer Series in Wood Science, IX + 254 S., 123 Figs., 20 Tab. Springer, Berlin-Heidelberg, 1984. ISBN 3-540-12574-4. Preis: DM 89. Feddes Repert. https://doi.org/10.1002/fedr.4910970721

Simpson WT (1998) Equilibrium moisture content of wood in outdoor locations in the united states and worldwide. For Prod Lab

Stagno V, Egizi F, Corticelli F, Morandi V, Valle F, Costantini G, Longo S, Capuani S (2021a) Microstructural features assessment of different waterlogged wood species by NMR diffusion validated with complementary techniques. Magn Reson Imaging. https://doi.org/10.1016/j.mri.2021.08.010

Stagno V, Genova C, Zoratto N, Favero G, Capuani S (2021b) Single-sided portable NMR investigation to assess and monitor cleaning action of PVA-borax hydrogel in travertine and Lecce stone. Molecules. https://doi.org/10.3390/molecules26123697

Stagno V, Mailhiot S, Capuani S, Galotta G, Telkki VV (2021c) Testing 1D and 2D single-sided NMR on Roman age waterlogged woods. J Cult Herit. https://doi.org/10.1016/j.culher.2021.06.001

Stagno V, Longo S, Capuani S (2020) Effect of age on Pine wood microstructure studied by micro-MRI and diffusion-NMR. 2020 IMEKO TC-4 Int Conf Metrol Archaeol Cult Herit 570–574

Thygesen LG, Tang Engelund E, Hoffmeyer P (2010) Water sorption in wood and modified wood at high values of relative humidity. Part I: results for untreated, acetylated, and furfurylated Norway spruce. Holzforschung. https://doi.org/10.1515/HF.2010.044

Thygesen LG, Elder T (2009) Moisture in untreated, acetylated, and furfurylated Norway spruce monitored during drying below fiber saturation using time domain NMR. Wood Fiber Sci

Tsoumis G (1991) Science and technology of wood. Structure, properties, utilization. Sci Technol wood Struct Prop Util